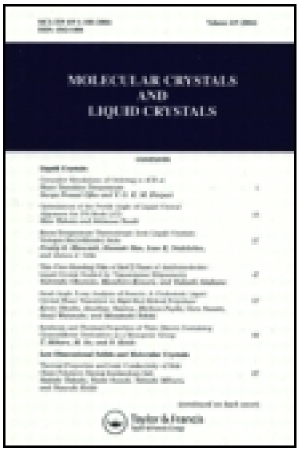

Molecular Crystals and Liquid Crystals Science and Technology. Section A. Molecular Crystals and Liquid Crystals

Publication details, including instructions for authors and subscription information:
http://www.tandfonline.com/loi/gmcl19

Formation and Dynamics of Convective Pattern in Homeotropic System of Nematic Liquid Crystals

Yoshiki Hidaka [a] , Ken-Ichi Hayashi [a] & Shoichi Kai [a]

[a] Department of Applied Science, Kyushu University, Fukuoka, 812-81, Japan

Version of record first published: 04 Oct 2006

Mol. Cryst. Liq. Cryst., 1997, Vol. 302, pp. 385-390
Reprints available directly from the publisher
Photocopying permitted by license only

FORMATION AND DYNAMICS OF CONVECTIVE PATTERN IN HOMEOTROPIC SYSTEM OF NEMATIC LIQUID CRYSTALS

YOSHIKI HIDAKA, KEN-ICHI HAYASHI AND SHOICHI KAI
Department of Applied Science, Kyushu University, Fukuoka, 812-81, Japan

Abstruct Pattern dynamics in a weakly nonlinear regime near the onset of the electrohydrodynamic instability (EHDI) is experimentally investigated in the homeotropic alignment of nematic liquid crystals, of which morphology is introduced. The wavy, chain and bamboo-chevron patterns are observed in homeotropic samples as new patterns. The Busse balloon is also obtained which is quite different from the conventional balloons in EHDI in planar liquid crystals.

INTRODUCTION

Electrohydrodynamic convection (EHC) is a typical self-organization phenomenon and one of the most convenient systems to investigate pattern formation in systems far from equilibrium.[1-4] In many past researches on this subject, much attention has been paid to a planar geometry because simple theoretical and experimental treatments can be possible,[3,4,5] in which the director is forced to be aligned parallel to glass substrates by rubbing treatments. Then EHC in the planar orientation occurs directly as a first instability from non-structural state. The basic research on EHC in the homeotropic nematics on the other hand was not active and systematic, because EHC occurs as a secondary instability after the orientational instability called the Freedericksz transition and because it was considered that there was not an essentially new phenomenon after the onset of EHC. Here the director aligns perpendicular to a glass substrate in homeotropic samples.

Very recently, however, by some of systematic works on homeotropic EHC there come out some important and new findings as well as theoretical progress, such as direct transition to the spatio-temporal chaos (STC) at the convective onset and new patterns such as chain, wavy and spiral patterns in weakly nonlinear regimes.[6-13] There is furthermore an experimental convenience in homeotropic EHC when the critical dynamics near the Lifshitz point is studied in detail because it can be easily and precisely controlled by the external magnetic field H. In a planar EHC contrary to this the detailed study near the Lifshitz point frequently requires the appropriate values of material constants such as the dielectric constants and conductivities. In addition, there is no experimental result on the Busse balloon in homeotropic EHC, although it is very important to understand the nonlinearity near the onset. Therefore the study on EHC in the homeotropic geometry becomes more attractive.[11-13]

In a present paper we will experimentally describe the nonlinear pattern formation in weakly nonlinear regimes and introduce the pattern morphology in the homeotropic nematics as well as the Busse balloon.

EXPERIMENTAL PREPARATION

We used the nematic liquid crystal *p*-methoxybenzilidene-*p*'-*n*-butylaniline (MBBA), which was filled between two glass plates both of which surfaces were coated with transparent electrodes, indium tin oxicide (ITO). The conductivity was $\sigma_{//} = 3.3 \times 10^{-7}\ \Omega^{-1}\mathrm{m}^{-1}$ and $\sigma_{\perp} = 2.3 \times 10^{-7}\ \Omega^{-1}\mathrm{m}^{-1}$ which was controlled using the 0.012 wt%-doping of tetra-*n*-butyle-ammonium bromide (TBAB). The dielectric constant was $\varepsilon_{//} = 4.21$ and $\varepsilon_{\perp} = 4.70$, *i.e.* $\varepsilon_a = -0.49$. The space between two glass plates was maintained by a polymer film with a separation of 50 μm and the lateral size was taken as $1 \times 1\ \mathrm{cm}^2$. Therefore the aspect ratio Γ of the convective systems in the present study was 200. In order to realize homeotropic alignments the surface of glass plates was treated by a surfactant (*n*-*n*'-dimethyl-*n*-octadecyl-3-aminopropyl-trimethoxysilyl chioride: DMOAP). The temperature was controlled within 30 ± 0.02 C° with a control stage and a double-wall copper cavity.

Without magnetic fields there is no preferred direction for convective rolls and therefore no specific direction (such as x and y) because of the continuous rotational symmetry. However when the magnetic field is applied parallel to the cell, the convective rolls align perpendicular to the direction of the magnetic field above V_c of which direction hereafter we set as x. Thus we could define the x-direction only in the presence of the magnetic field. In the present study, we conducted for $H = 1600$ G which was the intensity higher than the threshold $H_F = 1100$ G for a magnetically induced Freedericksz transition. The AC voltage was applied by an electronic synthesizer controlled by a computer. The threshold value for an electrically induced Freedericksz transition was about $V_F = 4$ V. We defined here the normalized external control parameter ε as $\varepsilon = (V^2 - V_c^2) / V_c^2$. The threshold for the onset of the convection was $V_c = 10$ V at $f = 500$ Hz and $H = 1600$ G. The critical frequency f_c of the applied electric field was about 2600 Hz. The detailed manner in order to obtain the Busse balloon was the conventional frequency-voltage jump method,[14-16] which has been already described elsewhere in detail.[17]

RESULTS AND DISCUSSION

The application of magnetic fields perpendicular to the director in the homeotropic nematics suppresses the Goldstone mode related to the azimuthal angle of the director and the preferred axis for the alignment is set up.[11] Here $H = 1600$ G was applied in order to suppress the Goldstone mode and to lead the preferred axis for the director orientation. Then the electric field was applied to induce the regular patterns in EHC. Figure 1 shows the pattern diagram after the occurrence of EHC in a frequency-voltage plane ranging from $f = 100$ Hz to 1900 Hz.[18]

In the low frequency regime ($f = 100 \sim 600$ Hz), near the first bifurcation point the

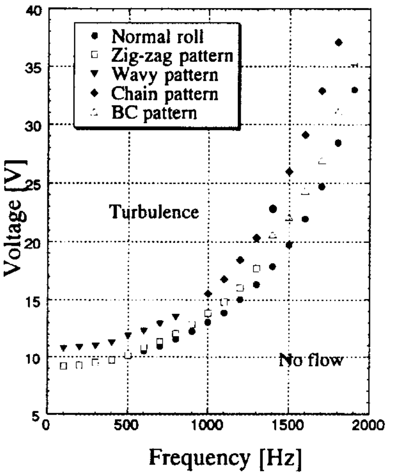

FIGURE 1 Phase diagram in the presence of magnetic fields (H = 1600 G).

zig-zag pattern is observed which is shown in Fig. 2a, as well as the frequency dependence of its tilted angle (obliqueness). This dependence does not agree well with theoretical predictions[12] and its tendency is rather similar to the previous experimental results by H. Richter.[6,7] Probably this may be due to the incomplete conditions, *e.g.* the measurement was not exactly achieved for the onset such as $\varepsilon = 0$ (linear regime) but for $\varepsilon = 0.01$ (weakly nonlinear regime) in order to observe at least visually. The theory may well describe the obliqueness in the planer EHC at the onset ($\varepsilon = 0$)[19] but might not perfectly in the homeotropic EHC by some reasons. Increasing in the driving voltage V the wavy pattern forms above the second threshold (Fig. 2b). Finally turbulence appears as V further increases. On the other hand, in the high frequency regime (f = 1400 ~ 1900 Hz), the normal roll is observed near the threshold as shown in Fig. 2c, and then bamboo-chevron (BC: Fig. 2d), chain patterns (Fig. 2e)[9] and finally turbulence are successively observed through several transitions with the well-defined thresholds. In the regime between them (f = 700 ~ 1300 Hz), turbulence starts via a chain pattern after the transition from the normal roll to the zig-zag pattern as V is raised from the convective onset. These different patterns appear with also well-defined thresholds as shown in Fig. 1.[20,21] All patterns are summarized in Fig. 1.

In EHC for planar alignments, there were several reports related to the Busse balloon.[15-17,22] However, there has been no report for EHC in homeotropic alignments because no regular pattern is observed at the onset in the absence of magnetic fields which makes us very difficult to determine both additional and secondary instabilities.[11] Therefore we applied the magnetic field H = 1600 G at the standard frequency f_0 = 800 Hz for the frequency-voltage jump method,[14-17] under which conditions a regular normal roll is observed at the onset. In a two dimensional planar system, we found basically three different selection dynamics for pattern formation such as (1) simple decay of rolls, (2) elastic relaxation of rolls by defects and (3) relaxation of rolls via an instability, and showed the clear Busse balloon.[17] In a two dimensional homeotropic system however the situation is slightly different. We found four different selection processes in total in addition to the above three, such as relaxation of rolls via successive two instabilities transiently, and therefore the Busse balloon becomes more complicated and quite different from a conventional balloon.

In Fig. 3 such a Busse balloon is shown where the finally stable pattern is a normal roll near the onset at the center. Here NS, E, ZZ and EZ indicate respectively the neutral

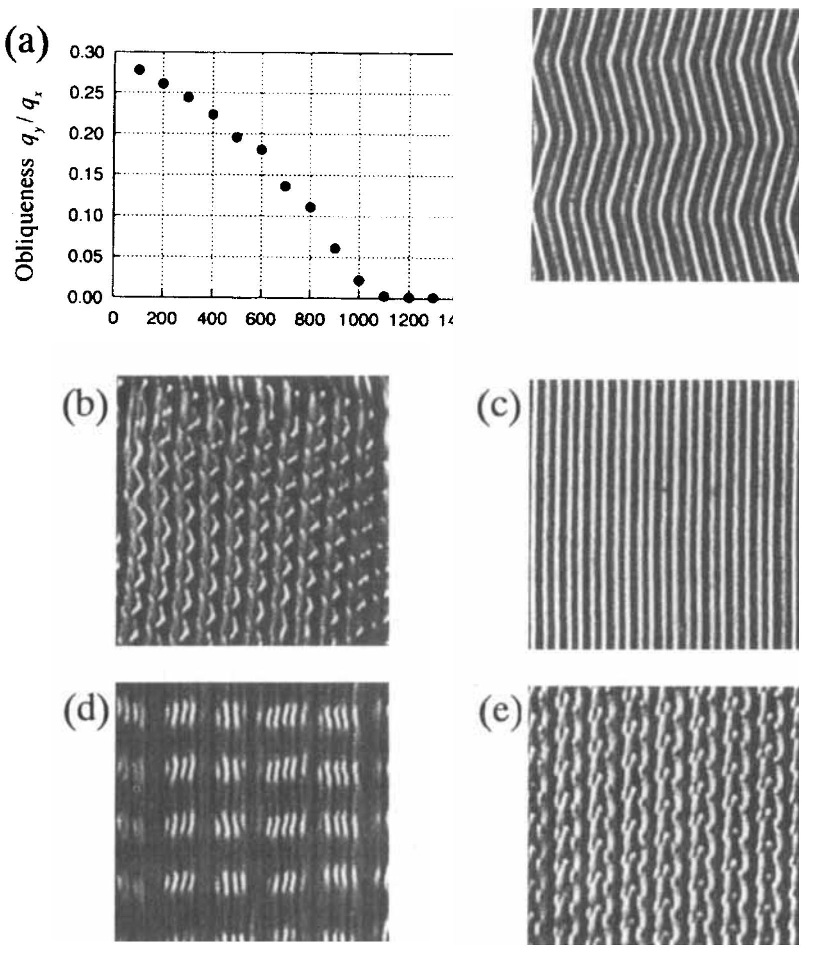

FIGURE 2 Typical patterns in the presence of H = 1600 G. The observation area is 400 × 400 μm². (a) zig-zag pattern. The upper figure shows the frequency dependence of the oblique angle of the zig-zag. (b) wavy pattern. (c) normal roll. (d) bamboo-chevron (BC) pattern. (e) chain pattern.

stability, the Eckhaus, the zig-zag and the Eckhaus-zig-zag boundaries. Below NS (♦), the rest state is stable. In the region I (○), the most favored pattern appears through the Eckhaus instability when the frequency-voltage jump is done. In the region II (×), the elastic relaxation of rolls due to elastic modifications and/or defect motions takes place. In the region III (○), the zig-zag pattern appears via the zig-zag instability. In the region IV (•), at the beginning the Eckhaus instability occurs and then the zig-zag pattern finally appears via the zig-zag instability. Each transient process is the following. In the Eckhaus instability (region I), the periodic defect creation/annihilation is observed. In the region II, no remarkable change of normal rolls is observed and small wavenumber modulation takes

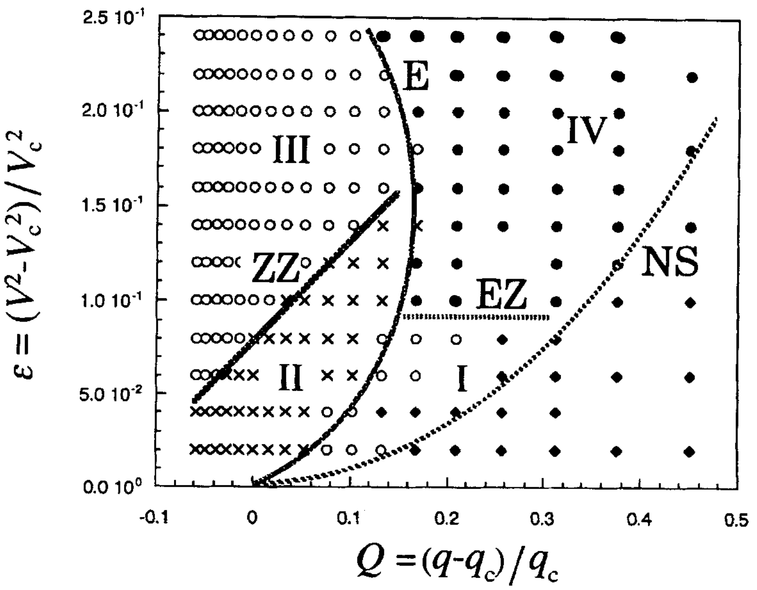

FIGURE 3 Busse balloon in homeotropic EHC with H = 1600 G. NS: neutral stability line, E: Eckhaus boundary, EZ: Eckhaus-zig-zag line, ZZ: zig-zag line (for detail see text).

place through elastic adjustments. In the region III, no remarkable change of the zig-zag pattern is observed after the frequency-voltage jump.

The most interesting fact is observed in the region IV where transiently two instabilities, the Eckhaus and the zig-zag ones, occur till the finally stable pattern forms. This could be explained by the scenario in Ref. 23. It should be mentioned that the Eckhaus (E) line bends back and the EZ line is parallel to the Q axis in our balloon. No theoretical prediction has been done on these.

SUMMARY

The Busse balloon in the presence of H was observed as well as various new patterns. Some patterns (wavy, BC patterns, propagating DSM) were newly found in this work. In the absence of H no Busse balloon was obtained. The phase diagram with H = 1600 G was determined for the homeotropic EHC which was quite different from that for planer EHC.

The Busse balloon obtained under H is not conventional. Especially the Eckhaus boundary has not simple profile and bends back about which no theory predicts. In some region in the balloon two successive instabilities (the Eckhaus and the zig-zag instabilities) occur for the pattern selection dynamics from initial to final patterns after the frequency-voltage jump. This suggests that after the frequency-voltage jump the system is Eckhaus unstable at the beginning and later changes into zig-zag unstable because the wavenumber approaches to $Q = 0$ where the state is zig-zag unstable.[23] Then the two successive transitions such as the Eckhaus and zig-zag instabilities are realized. It is therefore very interesting to investigate the profile of the Busse balloon as the frequency f_0 is changed. Each boundary must change because the observed pattern is varied with f. This is now in progress and will be reported elsewhere in near future.

The authors would like to thank M. I. Tribelsky (University of Tokyo), W. Pesch and A. Rossberg (University of Bayreuth) for valuable comments and stimulating discussions. This work is partly supported by the Grant-in-Aid for Scientific Research from Ministry of Education, Sport, Science and Culture in Japan.

REFERENCES

1. P.G. de Gennes, The Physics of Liquid Crystals, (Oxford University Press, New York, 1993) 2nd ed.
2. S. Kai and K. Hirakawa, Prog. Theor. Phys., supp. 68, 212 (1978).
3. S. Kai ed., Pattern Formation in Complex Dissipative Systems (World Sci. Pub. Singapore 1991).
4. L. Kramer, E. Bodenshatz, W. Pesch, W. Thom and W. Zimmermann, Liq. Cryst., 5, 699 (1989).
5. L. Kramer and W. Pesch, Annu. Rev. Fluid Mech., 27, 515 (1995).
6. H. Richter, N. Kloepper, A. Hertrich and A. Buka, Europhysics Lett., 30, 37 (1995); M. I. Tribelsky, K. Hayashi, Y. Hidaka and S. Kai, Proc. of the 1st Tohwa Univ. Stat. Phys. Meeting (1995).
7. A. Hertrich, Thesis (1995, Univ. of Bayreuth).
8. S. Kai and W. Zimmermann, Prog. Theor. Phys. supp. 99, 458 (1989); S. Kai, Y. Adachi and S. Nasuno, Spatio-Temporal Patterns, ed. P. E. Cladis and P. Palffy-Muhoray, (SFI Studies in the Sciences of Complexity, Addison-Wesley, 1995).
9. P. Cladis and C. Fradin who first observed and named it as a *chain pattern* (private communication in July of 1995).
10. H. Richter, A. Buka and I. Rehberg, Phys.Rev. E, 51, 5886 (1995).
11. S. Kai, K. Hayashi and Y. Hidaka, submitted to J. Phys. Chem..
12. A. Hertrich, W. Decker, W. Pesch and L. Kramer, J. Phys. (Paris) II, 2, 1915 (1992); and A. Rossberg, A. Hertrich, L. Kramer and W. Pesch, preprint (1996).
13. M. I. Tribelsky, Int.J.Bif.Chaos, (in print); M. I. Tribelsky and K. Tuboi, Phys. Rev. Lett., 76, 1631 (1996).
14. G. Goren, I. Procaccia, S. Rasenat and V. Steinberg, Phys. Rev. Lett., 63, 1237 (1989).
15. E. Braun, S. Rasenat and V. Steinberg, Europhys. Lett., 15, 597 (1991).
16. S. Nasuno and S. Kai, Europhys. Lett., 14, 779 (1991).
17. S. Nasuno, O. Sasaki, S. Kai and W. Zimmermann, Phys. Rev. A, 46, 4954 (1992).
18. K. Hayashi, Y. Hidaka and S. Kai, Proc. of the 1st Tohwa Univ. Satat. Phys. Meeting (1995).
19. M. Dennin, D. S. Cannell and G. Ahlers, Mol. Cryst. Liq. Cryst., 261, 337 (1995).
20. S. Kai, W. Zimmermann, M. Andoh and N. Chizumi, Phys. Rev. Lett., 64, 1111 (1990).
21. Y. Hidaka, K. Hayashi and S. Kai, in preparation.
22. M. Lowe and J. P. Gollub, Phys. Rev. Lett., 55, 2575 (1985); Phys. Rev. A, 31, 3893 (1985).
23. W. Pesch and A. Rossberg suggest us the interpretation about two successive instabilities (private communication). In region IV, rolls are only Eckhaus unstable and near the band center $Q = 0$ zig-zag unstable. Therefore the zig-zag instability will set in when it is reached. This leads to the succesive two instabilities.